



OPEN Gut microbiota from Mori fructus (*Morus alba* L.) polyphenols and polysaccharides-dosed mice activates the PPAR α /PGC-1 α signaling pathway to mitigate HFD-induced metabolic syndrome in mice

Meixia Wan^{1,2}✉, Qing Li², Yudie Xiao², Dan Zhou², Qianya Lei² & Shu Wang²

Mori Fructus, rich in polysaccharides and polyphenols, has long been used in East Asia as a functional food and medicinal agent. In traditional Chinese medicine, it is used to treat various ailments like wasting-thirst syndrome and constipation. Studies suggest its extract fractions may alleviate metabolic syndrome symptoms by affecting gut microbiota. To explore this, fecal microbiota transplantation (FMT) was used in an experiment. Pseudo-germ-free mice were created with antibiotics and given a high-fat, high-sugar diet (HFD) to induce metabolic syndrome. Then, fecal bacterial infusions were transplanted. Results showed significant improvement in metabolic syndrome parameters in the FMT-MFPS (fecal microbiota transplantation-Mori Fructus polyphenols plus polysaccharides) group. Dyslipidemia, liver, and kidney injuries were modulated in treated mice. The PPAR α /PGC-1 α signaling pathway was activated. These findings indicate Mori Fructus extract fractions prevent metabolic syndrome via gut microbiota modulation, with effects sustained through FMT, providing a reference for prevention.

Keywords Mori fructus (*Morus Alba* L.), Metabolic syndrome, Fecal microbiota transplantation, PPAR α /PGC-1 α signaling pathway

Abbreviations

FMT	Fecal microbiota transplantation
HFD	High-fat and high-sugar diet
MFP	Mori Fructus polyphenol-rich fraction
MFS	Mori Fructus polysaccharide-rich fraction
MFPS	Mori Fructus polyphenols plus polysaccharides
NCD	Normal chow diet
FMT-MFP	FMT from mice treated with MFP
FMT-MFS	FMT from mice treated with MFS
FMT-MFPS	FMT from mice treated with MFPS
AST	Aspartate aminotransferase
ALT	Alanine amino transferase
ELISA	Enzyme linked immunosorbent assay
MDA	Malondialdehyde
SOD	Superoxide dismutase
GSH-Px	Glutathione peroxidase

¹Medicine School, Longdong University, Qingyang 745000, China. ²West China School of Pharmacy, Sichuan University, Chengdu 610041, China. ✉email: wanmeixia2010@126.com

H&E	Hematoxylin and eosin
TC	Total cholesterol
TG	Triglyceride
LDL-C	Low density lipoprotein-cholesterol
HDL-C	High density lipoprotein-cholesterol
NAFLD	Nonalcoholic fatty liver disease
SCr	Serum creatinine
SUA	Serum uric acid
BUN	Blood urea nitrogen
IL-1 β	Interleukin-1 β
IL-6	Interleukin-6
TNF- α	Tumor necrosis factor- α
OGTT	Oral glucose tolerance test
AUC	Area under the curve
HOMA-IR	Homeostasis model assessment of insulin resistance
BCAAs	Branched chain amino acids
ANOVA	Analysis of variance

Metabolic syndrome in humans is a multifaceted condition characterised by multiple cardiovascular stressors, including overweight, insulin resistance, dyslipidemia, and hypertension¹. Furthermore, it represents a serious global health challenge, with increasing prevalence observed worldwide². Metabolic syndrome may lead to cardiovascular diseases such as atherosclerosis due to dysregulation of glucose and lipid metabolism³. Additionally, the presence of metabolic syndrome has been associated with Parkinson's disease, obstructive sleep apnea, renal carcinoma, colorectal cancer, or bladder cancer, severely impacting overall health^{3,4}. Current treatments for metabolic syndrome focus primarily on lifestyle changes, including regular physical activity and dietary changes, supplemented by pharmacological interventions and surgery².

Mori Fructus is naturally rich in polyphenols and polysaccharides, of which the main polyphenols are anthocyanins, rutin and chlorogenic acid⁵. These polyphenolic compounds act as natural reducing agents in the human body, exerting regulatory effects such as scavenging free radicals, anti-inflammatory, weight loss, anti-tumor, and prevention of metabolic disorders⁶. Plant polysaccharides as natural macromolecules have various benefits, including immune regulation, antioxidant activity, anti-inflammatory, anti-neoplastic, and antihyperglycemic effects⁷. The previous animal experiment has revealed that Mori Fructus extract fractions (Mori Fructus polyphenol-rich fraction, MFP; Mori Fructus polysaccharide-rich fraction, MFS; Mori Fructus polyphenols plus polysaccharides, MFPS) effectively alleviate metabolic syndrome and result in beneficial changes to gut ecology and profiles of faecal metabolites in mice⁸.

FMT, which entails transferring fecal microbiota from a healthy donor to a recipient, has attracted attention as a promising therapeutic strategy for a range of conditions, including metabolic syndrome^{9,10}. Currently, FMT treatment is recognised as one of the most straightforward and effective methods for reconstituting gut microbiota. Moreover, FMT treatment has been extensively approved in *Clostridioides difficile* infection¹¹. Since 2014, various diseases have been studied by FMT treatment globally, focusing on diseases such as *Clostridioides difficile* infection, irritable bowel syndrome, excess body weight, metabolic syndrome, hyperglycemic conditions, inflammatory intestinal disorders, ulcerative colitis, mood disorders, and hepatic dysfunctions¹². Recently, it has been noted that Chinese medicine possesses probiotic or prebiotic-like properties, which illustrates multi-component and polypharmacological effects of these therapeutic interventions, as viewed through the lens of intestinal microbial dynamics¹³.

Previous studies have revealed that probiotic-like regulation of gut microbiota was observed through the intervention of Mori Fructus extract fractions^{8,14}, but these effects have yet to be validated. The aim of this study was to investigate the mechanism of action of Mori Fructus extract fractions MFP, MFS, and MFPS in the amelioration of metabolic syndrome. Broad-spectrum antibiotic cocktail treatment was used to establish pseudo-germ-free mice, then a metabolic syndrome model in mice was induced by HFD. Simultaneously, faecal material from mice treated with MFP, MFS, and MFPS⁸ was orally administered to pseudo-germ-free mice, respectively¹⁵.

Materials and methods

Reagents

Ampicillin trihydrate (Lot#: C10752327), Vancomycin hydrochloride (Lot#: C10791656), and Streptomycin sulfate (Lot#: C12036834) were sourced from Macklin Biotechnology (Shanghai, China). Gentamycin sulfate (Product Number: G100391) was obtained from Aladdin Biotechnology (Shanghai, China).

Mori fructus extract fractions preparations

MFP, MFS, MFPS were prepared and characterized in the previous study⁸.

Design of experiments

Male C57BL/6J mice, weighing between 18 and 20 g, were procured from Dossy experimental animals technology in Chengdu, China, under the protocol designation SCXK (Chuan) 2020–030. Before the experiment began, mice were acclimated to specified pathogen-free conditions for eight days, housed in an environment with a temperature range of 22 \pm 2 °C and a humidity level of 50 \pm 5%.

The ethical clearance for all animal-based research was granted by Sichuan University Ethics Committee, situated in Chengdu, China, with the assigned protocol number SYXK (Chuan) 2018-113. The experimental

protocols were strictly in accordance with the European Community directives (86/609/EEC) concerning treatment and utilization of experimental animals. All methods are reported in accordance with ARRIVE guidelines.

Donor mice

Donor mice, preparing the fecal bacterial infusion solutions, were from the previous study⁸. Fecal samples were collected daily between 3:00 and 5:00 p.m. during the 14th experimental week. To minimize microbial contamination, all procedures were performed in a UV-sterilized laminar flow hood. Mice were gently restrained by pinching the back of the neck while stabilizing the tail, and slight abdominal pressure was applied to induce defecation. Fresh feces were immediately transferred to sterile cryopreservation tubes and flash-frozen in liquid nitrogen.

The preparation method for fecal bacterial infusion was optimised based on previous studies. Feces were homogenised in phosphate-buffered saline solution at a dilution ratio of 1:10 (weight to volume). The mixture was then subjected to centrifugation at 4 °C at a rotational speed of 3000 for 5 min. Supernatants were used as fecal bacterial infusion solutions, which were prepared for fresh daily use.

Recipient mice

The animal experiment protocol is shown in Fig. 1. Following an 8-day acclimatisation period, pseudo-germ-free mice were established. Mice were provided with drinking water supplemented with a combination of broad-spectrum antibiotics, including ampicillin trihydrate (0.5 mg/mL), streptomycin sulfate (1 mg/mL), vancomycin hydrochloride (0.5 mg/mL), and gentamicin sulfate (1 mg/mL). The antibiotic water was refreshed every two days, and mice were allowed to drink freely for 14 days.

A total of 30 pseudo-germ-free mice were grouped into five sets (6 mice per set, 3 mice for each cage): normal chow diet (NCD) group (received pure water, 0.2 mL/mouse), HFD group (received pure water, 0.2 mL/mouse), FMT-MFP group (FMT from mice treated with MFP, 0.2 mL/mouse), FMT-MFS group (FMT from mice treated with MFS, 0.2 mL/mouse), and FMT-MFPS group (FMT from mice treated with MFPS, 0.2 mL/mouse). Mice in the HFD and FMT intervention groups consumed a diet that was high in fat, comprising 45% of total caloric intake, which was obtained from Biotech Health Products Co., Ltd., Beijing, China. Additionally, the drinking water was supplemented with 4.2% fructose. Meanwhile, mice were provided with a diet that derived 15% of caloric content from fat in NCD group, obtained from Chengdu Dorsey Laboratory Animal Co. Ltd., Sichuan, China. They were also provided with purified drinking water. Fecal bacterial infusion solutions were administered by gavage between 9:00 a.m. and 11:00 a.m. every two days for 14 weeks, and body weights of mice were measured weekly. The changes in general conditions of mice in the whole experiment were observed, including mental status, diet, and hair.

Oral glucose tolerance test

On the 14th weekend of FMT treatment, mice were subjected to a 12 - hour continuous fast (from 21:00 h to 09:00 h), during which they consumed water uninterrupted. Subsequently, mice were gavaged with glucose at a dosage of 2 g·kg⁻¹. Then, blood samples were obtained from caudal vein at five time-points after gavage (0, 30, 60, 90 and 120 min) and the glycaemic levels were monitored with an ACCU-CHEK⁺ Performa Glucometer.

Sample collection

Euthanasia was performed in accordance with the guidelines established by the Institutional Animal Care and Use Committee (IACUC) and the American Veterinary Medical Association (AVMA). Mice were anesthetized using an intraperitoneal injection of a ketamine-xylazine mixture (100 mg/kg ketamine and 10 mg/kg xylazine). Following the induction of deep anesthesia, as confirmed by the absence of a pedal reflex, euthanasia was carried out by cervical dislocation. All efforts were made to minimize animal suffering during the procedure. Blood samples were obtained from orbital sinus of mice under anesthesia and subsequently subjected to centrifugation at 3000 rpm for 10 min at 4 °C to prepare for serum samples. Livers, kidneys, epididymal adipose tissue, and colons were rapidly excised, and the length of the colon was determined. Livers were homogenised with normal saline at a ratio of 1:10 (w/v) and the supernatants were separated by centrifugation. After the above steps, liver homogenates were obtained.

Biochemistry assays

Serum levels of AST, ALT, TC, TG, LDL-C, HDL-C, SCr, SUA and BUN were determined by the auto-biochemical analyser (Olympus AU400, Tokyo, Japan). Serum levels of insulin, IL-1 β , IL-6 and TNF- α were detected by ELISA kits (Thermo Fisher Scientific, Wilmington, DE, USA). Levels of MDA, SOD and GSH-Px in livers were quantified by commercially available assay kits (Nanjing Jiancheng Biotechnology, China).

Histological examination

Hepatic tissues, left renal lobes, proximal segments of colon, and epididymal adipose depots were preserved in a 4% paraformaldehyde solution, supplied by Servicebio in Wuhan, China, prior to being dissected for hematoxylin and eosin (H&E) staining. In a parallel procedure, the left hepatic lobes were subjected to Oil Red O staining to evaluate lipid deposition within liver. Histological specimens were stained and then photographed by an Olympus BX53 light microscope, a product of Olympus Corporation, Tokyo, Japan.

qRT-PCR

The RNA was extracted via an ultrapure RNA extraction kit (CW0581M, CWBIO), and the concentration and purity of the RNA were measured via a UV-visible spectrophotometer (NP80, NanoPhotometer) (OD260/

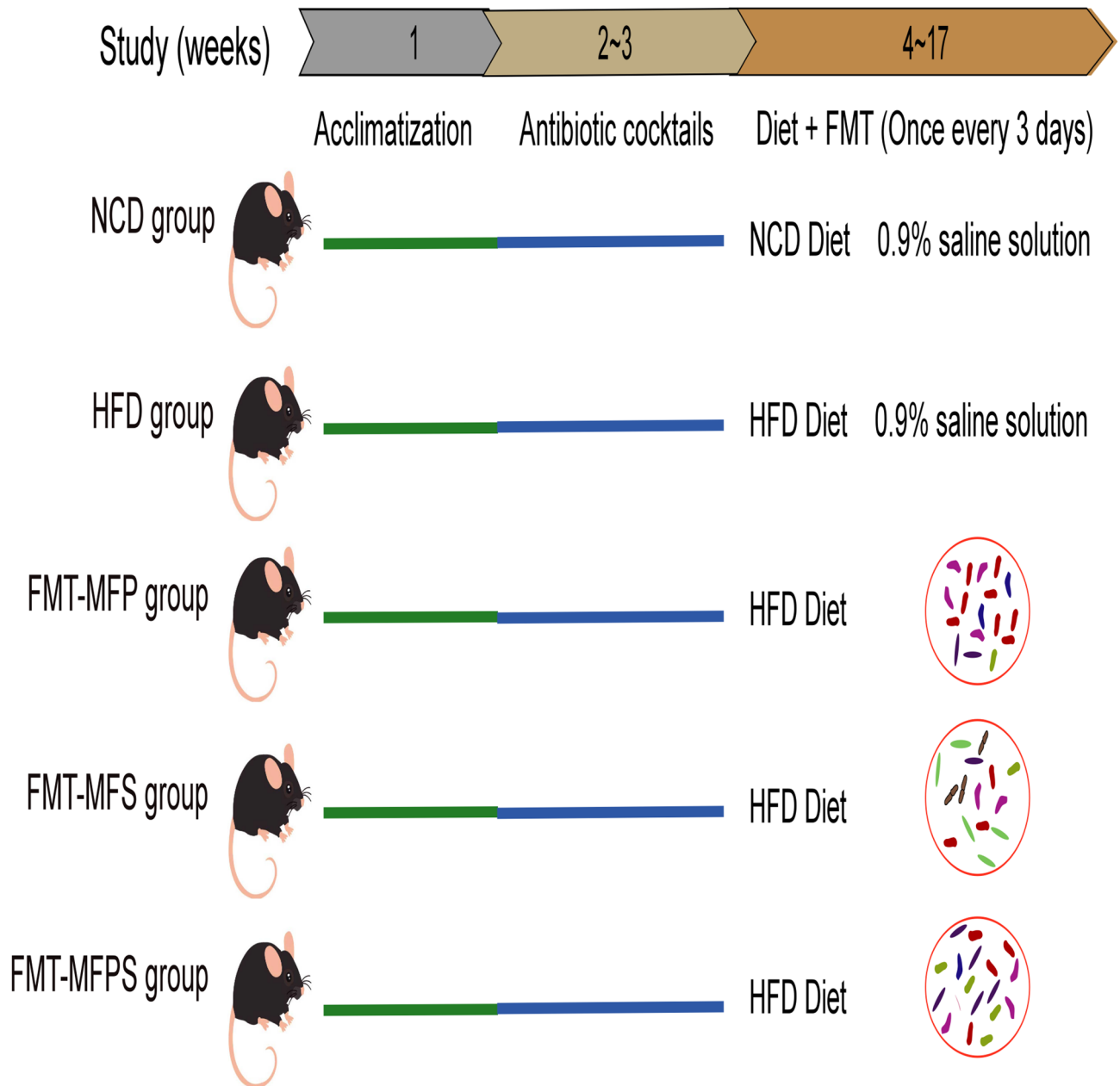


Fig. 1. The animal experimental protocol.

OD280). cDNA was synthesized via an RNA reverse transcription kit (R223-01, Vazyme), and fluorescence PCR was performed via a CFX Connect™ instrument. Real-time fluorescence quantitative PCR was performed using Bole Life Medical Products (Shanghai) Co., Ltd., and the relative expression levels of genes were calculated via the $2^{-\Delta\Delta Ct}$ method.

Western blot

Rabbit epidural scar tissue and VAF cells were collected, RIPA lysis buffer (C1053, ApplyGen) was added to the tissue, which was ground, the culture medium was discarded, and total protein was extracted with RIPA lysis buffer. The mixture was centrifuged at 12,000 rpm at 4 °C for 10 min, the supernatant was collected, and the total protein concentration was quantified via a BCA protein quantification kit (E-BC-K318-M, Elabscience). After denaturing the protein sample, sodium dodecyl benzene sulfonate gel electrophoresis (SDS-PAGE) was conducted, and a 300 mA constant flow membrane was used. After the PVDF membrane (Millipore) was blocked with skim milk powder, anti-GAPDH (TransGen Biotech, 1:2000), anti-PGC-1 α (abcam, 1:1000), anti-PPAR α (abcam, 1:1000), anti-PPAR γ (abcam, 1:1000), and anti-CPT-1 (abcam, 1:1000) antibodies were incubated overnight at 4 °C, and the next day, the secondary antibody IgG (H+L) (Servicebio, 1:2000) was incubated with the PVDF. The PVDF membrane was soaked with luminescent solution and placed in a highly

sensitive chemiluminescence imaging system (ChemiDocTMXRS+, Bole Life Medical Products (Shanghai) Co., Ltd.) for development.

Statistical analysis

Statistical analyses were performed by GraphPad Prism 7.0 and SPSS 20.0 and represented as arithmetic mean \pm standard error (SEM). Comparisons between sample data were performed by analysis of variance (ANOVA). Statistical significance was considered as $p < 0.05$.

Results

Behavioral changes

Mice had shiny fur, normal mental status, and active behavior in NCD and FMT-MFPS groups over a 14-week period. In contrast, mice had poor fur, increased water intake and urine output in HFD group.

Reduction in body weight and organ coefficient

Body weights were increasing in all groups over the 14-week feeding period (Fig. 2A). Compared with NCD group, body-weight gain, indexes of epididymal fat, liver and renal were highest in HFD group (Fig. 2B-E, $p < 0.01$ for all), and the HFD group had the shortest colon length (Fig. 2F, $p < 0.01$). Compared with the HFD group, the body-weight gain and epididymal fat index in FMT-MFPS group were markedly decreased ($p < 0.05$ and $p < 0.01$), FMT treatment significantly reduced the liver index ($p < 0.05$ for all), and the colon length was significantly increased in the FMT-MFPS group ($p < 0.01$). However, there was no significant change in renal indexes ($p > 0.05$). These results indicated that HFD increased the body weight and organ coefficient of mice, while FMT treatment significantly ameliorated the tissue damage in the FMT-MFPS group.

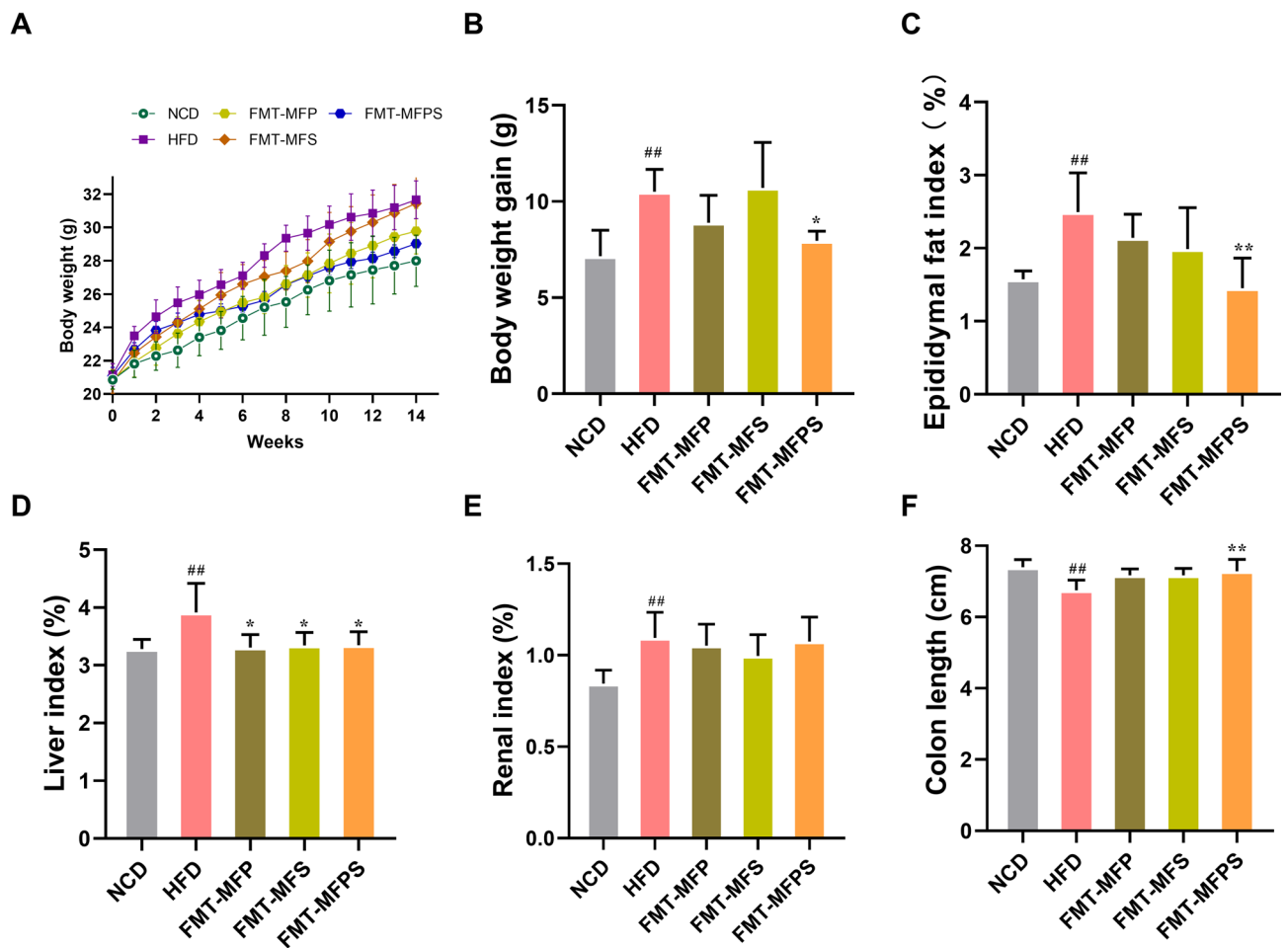


Fig. 2. Changes in body weight gain and organ coefficient of pseudo-germ-free mice in FMT intervention groups after 14 weeks of FMT treatment. (A) Body weight of mice and (B) body weight gain was shown in weeks during FMT treatment period. Ratios of epididymal adipose weight to body-weight (C), ratios of hepatic weight to body-weight (D), and ratios of renal weight to body-weight (E), colon length (F) were statistically analyzed via calculated using one-way ANOVA. # $p < 0.01$ compared to NCD group; * $p < 0.05$ and ** $p < 0.01$ compared to HFD group.

Regulatory influence on glucose metabolic dysregulation, lipid metabolism disorders and inflammation

The levels of OGTT-AUC, FBG, fasting serum insulin and HOMA-IR were markedly elevated in HFD group (Fig. 3A-D, $p < 0.01$ for all), indicating that HFD induced glucose metabolism disorders. In comparison to HFD group, FBG decreased significantly in FMT-MFPS group (Fig. 3A, $p < 0.05$). Moreover, OGTT was significantly reduced by FMT treatment in FMT-MFP and FMT-MFPS groups (Fig. 3B, $p < 0.01$ for all). Levels of serum insulin and HOMA-IR (Fig. 3C-D, $p < 0.01$ for all) were markedly reduced by FMT treatment in FMT-MFP, FMT-MFS and FMT-MFPS groups, suggesting that FMT treatments ameliorated HFD-induced glucose metabolism disorders.

In comparison to NCD group, serum levels of TC, TG, LDL and VLDL were markedly elevated (Fig. 3E-H, $p < 0.01$ for all). Additionally, serum levels of HDL showed a decreasing trend in HFD group (Fig. 3I, $p > 0.05$), suggesting that HFD induced dyslipidemia in mice. In comparison to HFD group, serum levels of TG, TC and LDL were markedly decreased in FMT-MFP and FMT-MFPS groups ($p < 0.01$ and $p < 0.05$). Furthermore, in FMT-MFS group, serum concentrations of TG were markedly decreased (Fig. 3E, $p < 0.01$), and serum levels of HDL were significantly increased in the FMT-MFS and FMT-MFPS groups (Fig. 3I, $p < 0.05$ for all). These results indicated that FMT treatment improved HFD-induced lipid metabolism disorders in FMT-MFP and FMT-MFPS groups, and the modulating effects were more pronounced in FMT-MFPS group.

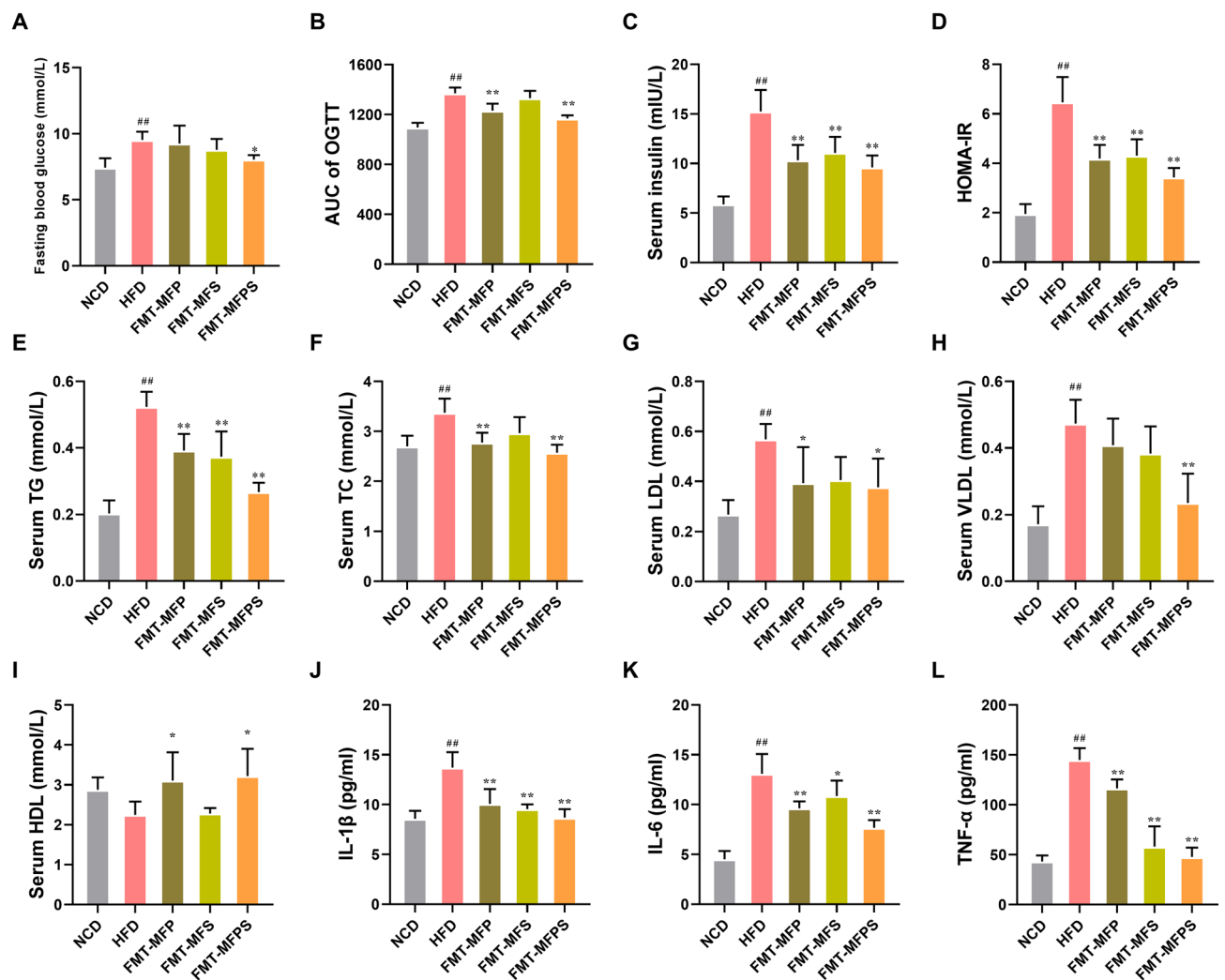


Fig. 3. FMT treatment prevented glucose metabolic dysregulation, lipid metabolism disorders and inhibit Inflammation. (A) OGTT experiments were performed and blood glucose values were measured at each time point before mice were executed, AUC of OGTT was calculated. (B,C) FBG and fasting serum insulin were assayed using a glucometer and ELISA kits, respectively. (D) HOMA-IR were calculated. (E–I) Serum levels of TG, TC, LDL-C, VLDL-C and HDL-C were assessed with an automated biochemical analyzer. Serum levels of IL-1 β (J), IL-6 (K) and TNF- α (L) were quantified with ELISA kits. Data were statistically analyzed by one-way ANOVA. ## $p < 0.01$ compared to NCD group; * $p < 0.05$ and ** $p < 0.01$ compared to HFD group.

Serum levels of IL-1 β , IL-6, and TNF- α were markedly upregulated in HFD group ($p < 0.01$), whereas those levels were significantly reduced in FMT-MFP, FMT-MFS and FMT-MFPS groups by FMT treatment (Fig. 3J-L, $p < 0.05$ and $p < 0.01$). This suggested that FMT treatment suppressed inflammatory cytokines.

Beneficial effects on liver and renal function and oxidative stress

Compared with NCD group, activities of AST and ALT were markedly upregulated in HFD group (Fig. 4A-B, $p < 0.01$ for all). Compared with HFD group, activities of ALT in serum were markedly decreased by FMT treatment ($p < 0.01$ for all) in FMT-MFP, FMT-MFS, and FMT-MFPS groups, and the AST level was significantly decreased in the FMT-MFPS group ($p < 0.01$). It was shown that FMT treatment in FMT-MFPS group could improve the liver function.

In comparison with NCD group, serum concentrations of SCr, BUN and SUA, were remarkably elevated in HFD group (Fig. 4C-E, $p < 0.01$ and $p < 0.05$). When compared to HFD group, serum concentrations of SCr were markedly decreased by FMT treatment ($p < 0.01$ for all) in FMT-MFP, FMT-MFS, and FMT-MFPS groups, at the same time, serum concentrations of BUN and SUA were decreased in FMT-MFS and FMT-MFPS groups ($p < 0.05$ and $p < 0.01$). These results indicated that FMT treatment improved renal function in FMT-MFS and FMT-MFPS groups.

Compared with NCD group, MDA levels in liver tissue were markedly induced (Fig. 4F) ($p < 0.01$), while the activities of SOD and GSH-Px were significantly decreased in HFD group (Fig. 4G-H, $p < 0.01$). When compared to HFD group, the levels of MDA in FMT-MFP, FMT-MFS and FMT-MFPS groups were significantly decreased ($p < 0.01$ for all), while the levels of SOD and GSH-Px in FMT-MFS and FMT-MFPS groups were significantly increased ($p < 0.01$ and $p < 0.05$). These findings suggested that FMT treatment was able to improve liver and kidney function and inhibit oxidative stress in FMT-MFPS group.

Improvement effect on tissue injury

H&E staining analysis revealed an increase in epididymal adipocyte volume in HFD group. While it was decreased in FMT-MFPS group, similar to NCD group (Fig. 5A). The results indicated that HFD induced a remarkable increase in fat accumulation, whereas FMT treatment significantly reduced these changes in FMT-MFPS groups.

Liver tissue was examined by H&E staining and Oil Red O staining are illustrated in Fig. 5B and 5C. Liver lipid droplets of mice were notably reduced in FMT-MFP, FMT-MFS and FMT-MFPS groups. Meanwhile, a limited number of lipid droplets were observed in the liver of FMT-MFPS group, indicating a return to normal hepatic morphology. These data demonstrate that FMT treatment effectively reduced hepatic fat deposition in FMT-MFP, FMT-MFS and FMT-MFPS groups, with the most pronounced improvement observed in FMT-MFPS group.

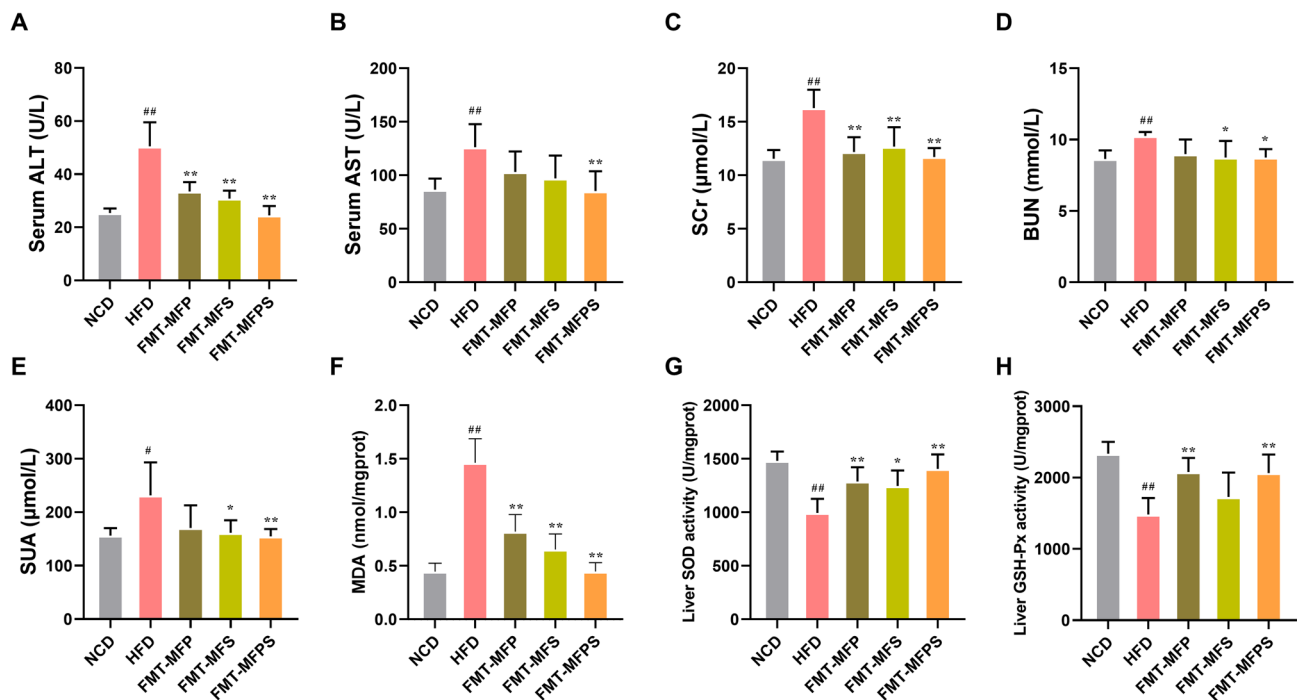


Fig. 4. FMT treatment improved liver and kidney function and inhibit oxidative stress. (A) ALT, (B) AST, (C) SCr, (D) BUN and (E) SUA, were quantified by an automated biochemical analyzer. The concentrations of MDA (F), SOD (G) and GSH-Px (H) of liver tissues were assessed through commercially available assay kits. # $p < 0.05$ and ## $p < 0.01$ compared to NCD group; * $p < 0.05$ and ** $p < 0.01$ compared to HFD group.

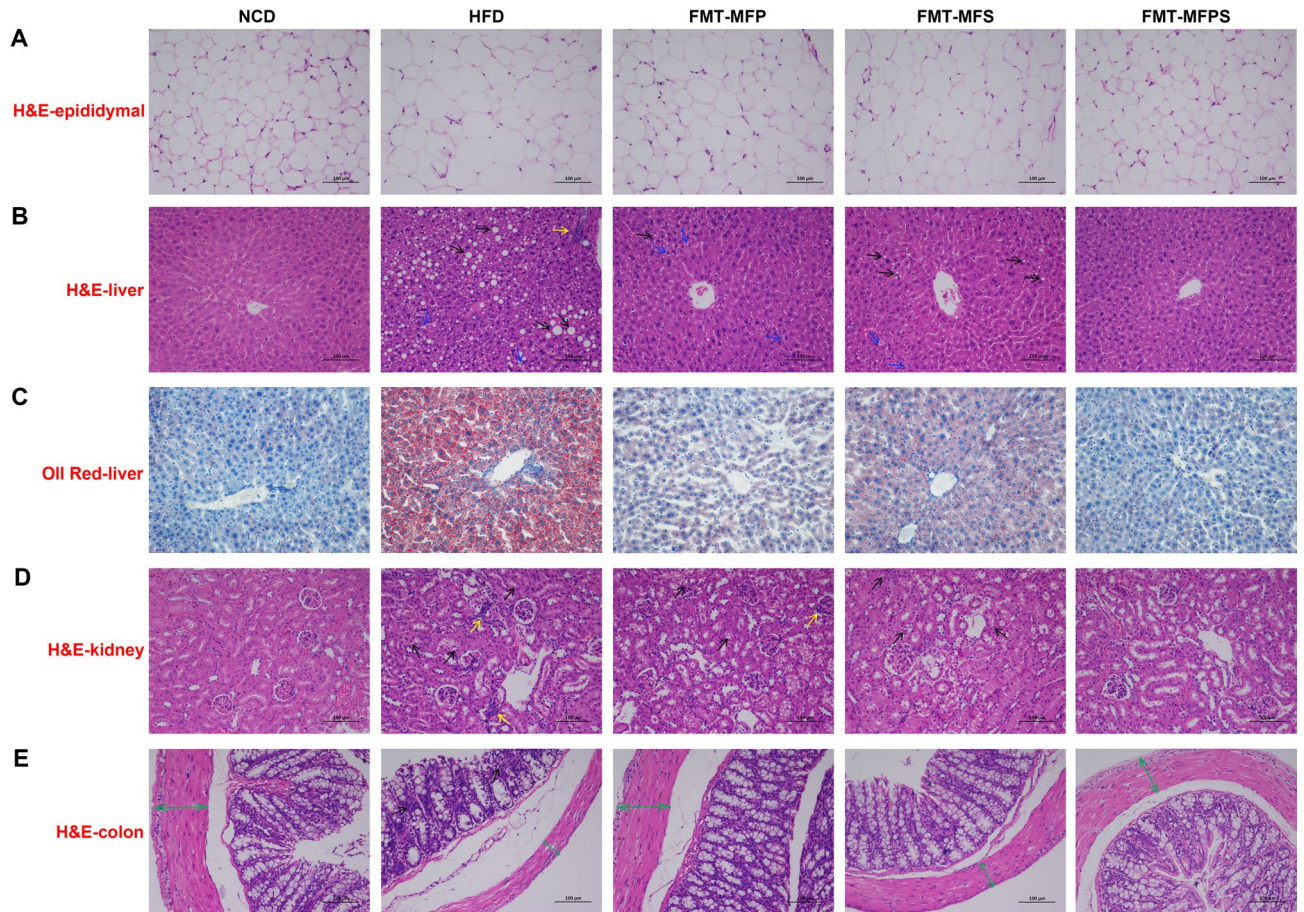


Fig. 5. Pathological staining of different tissues. **(A)** Photomicrographs of epididymal adipose tissue were obtained at a magnification of 200x using H&E staining. Liver tissue sections were subjected to H&E **(B)** and Oil Red O **(C)**, and microstructures were visualized at a magnification of $\times 200$, respectively. The presence of lipid droplet formation is indicated by black arrows, while fatty degeneration with edema is denoted by blue arrowheads. Additionally, the presence of inflammatory cell infiltration is highlighted by yellow arrows. **(D)** Kidney tissue sections were stained with H&E and microstructures were visualized at $\times 200$ magnification. The presence of diffuse swelling is indicated by black arrows, and the presence of inflammatory cell infiltration is highlighted by yellow arrows. **(E)** H&E - stained micrographs of colon tissue were observed at $\times 200$ magnification. Black arrows represent the presence of inflammatory cell infiltration, and green arrows indicate colonic muscularis propria.

The renal tubular epithelium exhibited diffuse mild swelling, slight inflammatory cell infiltration, and mild necrosis and detachment, indicating that kidneys probably had lipid lesions in HFD group (Fig. 5D). After 14 weeks of FMT treatment, diffuse swelling of kidneys was ameliorated, and renal histomorphological characteristics were predominantly restored to a near-normal morphology in FMT-MFPS group. These results indicated that FMT treatment alleviated renal injury in both FMT-MFP and FMT-MFPS groups.

H&E staining revealed that the proximal colon mucosa showed a small amount of inflammatory cell infiltration, a normal depth of crypts, and no obvious abnormality in intestinal wall, reflecting a typical colon morphology in NCD group. In contrast, proximal colonic tissue exhibited severe disruption, as evidenced by thinning of the colonic muscularis propria, reduced goblet cells, abnormal crypt structure, and increased inflammatory cell infiltration in HFD group (Fig. 5E). The thickness of the colonic muscularis layer was increased and the inflammatory state was attenuated in FMT-MFP, FMT-MFS, and FMT-MFPS groups, indicating that FMT treatment effectively mitigated colonic lesions induced by HFD.

Regulation of PPAR α /PGC-1 α signaling pathway

As shown in Fig. 6A-I, the mRNA and protein levels of PGC-1 α , PPAR α , PPAR γ , and CPT-1, which are associated with the PPAR α /PGC-1 α signaling pathway, were quantified using qPCR and Western blotting. Compared to the NCD group, the HFD group exhibited a significant reduction in the mRNA and protein levels of these markers ($p < 0.01$). Following FMT treatment, both the FMT-MFS and FMT-MFPS groups showed a significant increase in the mRNA and protein levels of PGC-1 α , PPAR α , PPAR γ , and CPT-1 compared to the HFD group ($p < 0.01$). Notably, within the FMT-MFP group, the mRNA levels of PGC-1 α , PPAR α , and CPT-1, as well as the protein level of CPT-1, were significantly elevated relative to the HFD group ($p < 0.05$ and $p < 0.01$). These

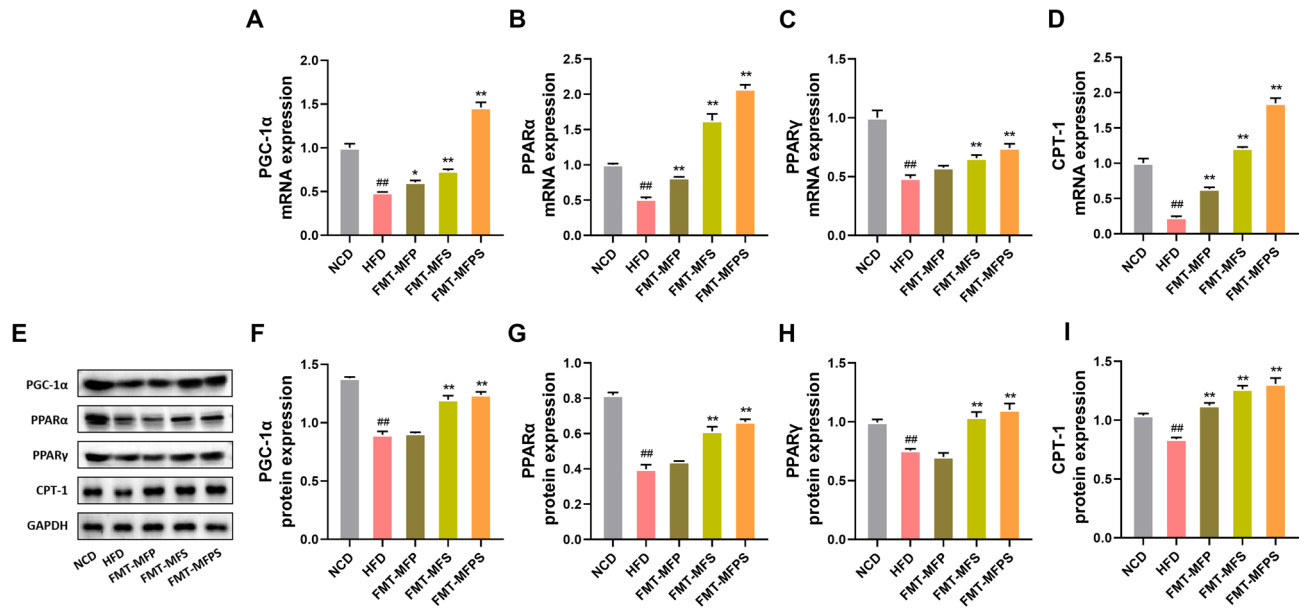


Fig. 6. FMT treatment activates PPAR α /PGC-1 α signaling pathway. mRNA expression levels of (A) PGC-1 α , (B) PPAR α , (C) PPAR γ , and (D) CPT-1. (E) Western blot detection strip. (F) PGC-1 α , (G) PPAR α , and (D) CPT-1. (H) PPAR γ , and (I) CPT-1 protein expression levels. ## p < 0.01 compared to NCD group; * p < 0.05 and ** p < 0.01 compared to HFD group.

findings suggest that HFD downregulates the expression of molecules in the PPAR α /PGC-1 α signaling pathway, whereas FMT treatment can effectively reverse this suppression.

Discussion

Germ-free mice or pseudo-germ-free mice are commonly used for FMT experiments¹⁵. Germ-free mice are those that have been kept in an aseptic environment from birth (aseptic cesarean section) and are provided with a strictly aseptic diet. Additionally, a series of techniques are employed to regularly monitor their sterile environment¹⁶. Therefore, germ-free mice are not only expensive but also have harsh breeding conditions, requiring more training and financial resources¹⁷. In addition, germ-free mice, which have an incompletely developed immune system with low immunity, are typically utilized for research on specified or well-characterized gut microorganisms¹⁸. Pseudo-germ-free mice are obtained through the administration of a mixture of broad-spectrum antibiotics, which effectively eliminates the majority of gut microbiota. This approach provides several advantages, including a well-developed immune system, ease of accessibility, and cost-effectiveness¹⁹. It was demonstrated that eradication of the intestinal microbiota was up to 90% when treated with a combination of broad-spectrum antibiotics^{19,20}. The appearance characteristics, behavior, physiological indexes and organ development indexes of pseudo-germ-free mice are similar to those of SPF mice, and the research results on gut microbiota are reliable^{21,22}. Therefore, a mixture of broad-spectrum antibiotics was used to establish pseudo-germ-free mice as experimental animals for FMT experiments. Then, a metabolic syndrome model of mice was constructed by methods of previous studies⁸.

Gut microbiota dysbiosis has been implicated in metabolic disorders related to obesity, diabetes mellitus, and non-alcoholic fatty liver disease (NAFLD)²³. A previous study also demonstrated that gut microbiota structure and metabolites were dysregulated in HFD-induced mice. After the interventions with Mori Fructus extracts, gut microbiota structure and metabolites in mice were adjusted¹⁸. Studies demonstrate distinct sex-based differences in lipid metabolism, which correlate with gut microbiota composition. Male and female mice with intact microbiota exhibit sex-specific variations in lipid metabolism gene expression, whereas germ-free mice show more pronounced sex differences in genes associated with intestinal health and inflammatory response²⁴. FMT is emerging as a prospective therapeutic intervention aimed at manipulating gut microbiota in various chronic diseases. Research has revealed that FMT treatment improved metabolic syndrome, obesity, hyperlipidaemia, inflammatory cytokines, and elevated insulin sensitivity index in clinical trials and animal experiments²⁵. Consequently, FMT treatment was employed to verify whether MFP, MFS or MFPS play an important role in ameliorating metabolic syndrome by modulating gut microflora or metabolites.

In this study, notable alterations in pharmacologic parameters were observed in HFD group when compared with NCD group. These changes included a substantial increase in body weight (p < 0.01), notable increases in organ weight indexes (epididymal adipose tissue, hepatic tissue, and renal tissue) (p < 0.01), and markedly elevated concentrations of FBG (p < 0.01). Furthermore, there were significantly elevated levels of fasting serum insulin and HOMA-IR (p < 0.01 for both). Additionally, levels of TC, TG, LDL-C, and VLDL-C were significantly increased (p < 0.01). These findings indicated successful establishment of metabolic syndrome model in mice induced by HFD.

Treatment with FMT derived from MFPS-treated mice significantly ameliorated symptoms of metabolic syndrome in FMT-MFPS group. These improvements included prevention of body weight gain and fat accumulation (Figs. 2B and 5A), reduction of hepatic fat deposition (Fig. 5B-C), alleviation of oxidative stress (Fig. 4F-H), amelioration of glucose and lipid metabolism disorders (Fig. 3A-I), mitigation of renal injury (Fig. 5D) and proximal colon injury (Fig. 5E). After transplanting the fecal bacteria from mice treated with MFP and MFS, the symptoms of metabolic syndrome of mice were ameliorated to some extent, but the preventive effects were not as good as those of FMT-MFPS group.

Levels of LDL-C, OGTT-AUC, and liver index were significantly elevated in FMT-MFP group, whereas levels of HDL-C and activities of GSH-Px were markedly reduced. These findings indicated that FMT treatment exerts regulatory effects on lipid abnormalities and liver injury in FMT-MFP group. The levels of OGTT-AUC, SUA and BUN were significantly reduced in FMT-MFS group, revealing that FMT treatment has modulatory effects on renal injury.

Gut microbiota is the most abundant and complex microbiome in humans, offering noteworthy metabolic and immune beneficial effects for the host²⁶. The motivation for epidemiological studies of gut microbiota in obesity and metabolic syndrome emerged from rodent studies demonstrating links among the gut microbiota, adiposity, and glucose tolerance. Metabolic dysfunctions related to metabolic syndrome, including chronic inflammation, hyperglycaemia and hyperlipidaemia, lead to gut microecological dysregulation²⁷. Previous research has shown that HFD induces a characteristic gut microbiota composition in mice, suggesting the potential of FMT-derived gut microbiota for the treatment of HFD-induced metabolic dysfunction⁸.

Peroxisome proliferator-activated receptor gamma coactivator-1 α (PGC-1 α) is a key regulator of energy metabolism. It responds to environmental stimuli and nutritional signals and interacts with various transcription factors to regulate multiple physiological processes, including glucose metabolism, lipid metabolism, and the biological clock²⁸. In high-fat diet (HFD)-induced metabolic disorders, PGC-1 α helps improve metabolic disorders by activating the transcription of fat oxidation genes in mitochondria and peroxisomes and increasing fatty acid oxidation²⁹. Additionally, PGC-1 α is involved in regulating hepatic gluconeogenesis and mitochondrial ATP biosynthesis, playing a crucial role in maintaining energy balance and glucose and lipid metabolism³⁰. PGC-1 α can be activated by PPAR α and PPAR γ and acts as their coactivator to enhance mitochondrial biogenesis and energy metabolism³¹.

Peroxisome proliferator-activated receptors (PPARs) are a class of ligand-dependent nuclear transcription factors, including three subtypes: PPAR α , PPAR β/δ , and PPAR γ . They form heterodimers with retinoid X receptors (RXRs) upon ligand binding and then bind to PPRE (peroxisome proliferator response elements) on DNA to regulate the expression of target genes³². PPAR α and PPAR γ are important transcriptional regulators of lipid metabolism, participating in peroxisomal β -oxidation, mitochondrial β -oxidation, fatty acid transport, and hepatic glucose production³⁰. In HFD-induced metabolic disorders, PPAR α reduces the incidence of liver steatosis by enhancing the expression of fatty acid oxidation genes and negatively regulates signaling pathways related to pro-inflammatory responses, thereby alleviating inflammation; PPAR γ , upon ligand binding, interacts with coactivators or corepressors to regulate the expression of downstream genes, modulating fat metabolism, inflammatory responses, cell differentiation, and energy balance³³. Research has demonstrated that lactic acid bacteria disrupt fatty acid oxidation by altering intestinal structure and suppressing the expression of lipid metabolism genes PPAR α and PGC-1 α ³⁴. In contrast, *Escherichia coli* RB01 generates acetate that intestinal cells convert into acetyl-CoA and AMP, subsequently activating the AMPK/PGC-1 α /PPAR α pathway and enhancing β -oxidation³⁵.

Carnitine palmitoyltransferase-1 (CPT-1) is a key enzyme in fatty acid β -oxidation, catalyzing the transfer of long-chain fatty acids from acyl-CoA to carnitine, thereby facilitating the entry of fatty acids into mitochondria for oxidation. In HFD-induced metabolic disorders, the expression and function of the CPT-1 gene are significantly affected. For instance, in an HFD-induced non-alcoholic fatty liver disease (NAFLD) model, the expression of CPT-1 is significantly reduced, leading to decreased fatty acid oxidation and increased accumulation of fatty acids in the liver³⁶. Studies have shown that the expression and activity of the CPT-1 gene can be regulated by PPAR α and PGC-1 α . PPAR α and PGC-1 α activate the transcription of the CPT-1 gene through different gene elements. PGC-1 α can activate the CPT-1 gene through independent gene elements without relying on the binding sites of PPAR α ; PPAR γ regulates the expression of the CPT-1 gene through its binding sites in the CPT-1 gene, thereby promoting fatty acid oxidation and improving lipid metabolism and oxidative stress^{37,38}. In the study, the PPAR α /PGC-1 α signaling pathway was significantly inhibited in the HFD group and activated after FMT treatment (Fig. 6), suggesting that FMT may exert therapeutic effects through the PPAR α /PGC-1 α signaling axis, which requires further verification.

Conclusions

In this study, a combination of broad-spectrum antibiotics was utilized to establish pseudo-germ-free mice, which were subsequently subjected to a HFD to establish mice model of metabolic syndrome. Subsequent transplantation of fecal bacterial solution from mice treated with MFPS resulted in a significant amelioration of various symptoms associated with metabolic syndrome. These improvements include reduction in weight gain, attenuation of hepatic steatosis, suppression of oxidative stress, modulation of dysregulated glucose and lipid metabolism, and mitigation of renal impairment and colonic damage. Similarly, there was a slight improvement in the manifestations of metabolic syndrome after FMT from mice treated with MFP or MFS to the corresponding recipient groups (FMT-MFP, FMT-MFS groups). After FMT treatment, levels of LDL-C, OGTT-AUC and liver index were significantly reduced, and levels of HDL-C and activities of GSH-Px were elevated in mice of FMT-MFP group, suggesting that transplantation of fecal bacterial solution from mice treated with MFP had a regulatory effect on dyslipidemia and liver injury. Levels of OGTT-AUC, SUA and BUN were significantly reduced in mice of FMT-MFS group, suggesting that FMT treatment had modulating

effects on renal injury in FMT-MFS group. The expression of genes related to PPAR α /PGC-1 α signaling pathway was up-regulated, suggesting that FMT may act through PPAR α /PGC-1 α signaling pathway. In conclusion, the findings suggested that polyphenol and polysaccharide fractions of Mori Fructus retain significant preventive efficacy when administered by FMT treatment. It highlights the important reference value of these fractions in elucidating the pharmacological mechanisms of Mori Fructus extract fractions (MFP, MFS, MFPS) in preventing metabolic syndrome.

Data availability

The data presented in this study are available on request from the corresponding author.

Received: 3 March 2025; Accepted: 25 July 2025

Published online: 01 August 2025

References

1. Takeuchi, T. et al. Gut microbial carbohydrate metabolism contributes to insulin resistance. *Nature* **621**, 389–395. <https://doi.org/10.1038/s41586-023-06466-x> (2023).
2. Saklayen, M. G. The global epidemic of the metabolic syndrome. *Curr. Hypertens. Rep.* **20**, 12. <https://doi.org/10.1007/s11906-018-0812-z> (2018).
3. Hsu, C. N., Hou, C. Y., Hsu, W. H. & Tain, Y. L. Early-Life origins of metabolic syndrome: mechanisms and preventive aspects. *Int. J. Mol. Sci.* **22** <https://doi.org/10.3390/ijms222111872> (2021).
4. Nagel, G. et al. Metabolic factors and the risk of small intestine cancers: pooled study of 800 000 individuals in the metabolic syndrome and cancer project. *Int. J. Cancer.* **149**, 66–74. <https://doi.org/10.1002/ijc.33530> (2021).
5. Ping-Ping, W., Wen-Duo, W., Chun, C., Xiong, F. & Rui-Hai, L. Effect of fructus mori. Bioactive polysaccharide conjugation on improving functional and antioxidant activity of Whey protein. *Int. J. Biol. Macromol.* **148**, 761–767. <https://doi.org/10.1016/j.jbiomac.2020.01.195> (2020).
6. Luca, S. V. et al. Bioactivity of dietary polyphenols: the role of metabolites. *Crit. Rev. Food Sci. Nutr.* **60**, 626–659. <https://doi.org/10.1080/10408398.2018.1546669> (2020).
7. Kasprzak-Drozd, K., Oniszczuk, T., Stasiak, M. & Oniszczuk, A. Beneficial effects of phenolic compounds on gut microbiota and metabolic syndrome. *Int. J. Mol. Sci.* **22** <https://doi.org/10.3390/ijms22073715> (2021).
8. Wan, M., Li, Q., Lei, Q., Zhou, D. & Wang, S. Polyphenols and polysaccharides from *Morus Alba* L. Fruit attenuate High-Fat Diet-Induced metabolic syndrome modifying the gut microbiota and metabolite profile. *Foods* <https://doi.org/10.3390/foods11121818> (2022).
9. Porcari, S. et al. Key determinants of success in fecal microbiota transplantation: from Microbiome to clinic. *Cell. Host Microbe.* **31**, 712–733. <https://doi.org/10.1016/j.chom.2023.03.020> (2023).
10. Tie, Y. et al. Current insights on the roles of gut microbiota in inflammatory bowel disease-associated extra-intestinal manifestations: pathophysiology and therapeutic targets. *Gut Microbes.* **15**, 2265028. <https://doi.org/10.1080/19490976.2023.2265028> (2023).
11. Weingarden, A. R. & Vaughn, B. P. Intestinal microbiota, fecal microbiota transplantation, and inflammatory bowel disease. *Gut Microbes.* **8**, 238–252. <https://doi.org/10.1080/19490976.2017.1290757> (2017).
12. Singh, P. et al. Effect of antibiotic pretreatment on bacterial engraftment after fecal microbiota transplant (FMT) in IBS-D. *Gut Microbes.* **14**, 2020067. <https://doi.org/10.1080/19490976.2021.2020067> (2022).
13. Huang, M., Cople-Rodrigues, C., Waitzberg, D. L., Rocha, I. & Curioni, C. C. Changes in the gut microbiota after the use of herbal medicines in overweight and obese individuals: A systematic review. *Nutrients* <https://doi.org/10.3390/nu15092203> (2023).
14. Chen, C. et al. Modulation of gut microbiota by mulberry fruit polysaccharide treatment of obese diabetic db/db mice. *Food Funct.* **9**, 3732–3742. <https://doi.org/10.1039/c7fo01346a> (2018).
15. Li, J., Huang, H., Fan, R., Hua, Y. & Ma, W. Lipidomic analysis of brain and hippocampus from mice fed with high-fat diet and treated with fecal microbiota transplantation. *Nutr. Metab.* **20**, 12. <https://doi.org/10.1186/s12986-023-00730-7> (2023).
16. Lauko, S. et al. Beneficial effect of faecal microbiota transplantation on mild, moderate and severe dextran sodium Sulphate-Induced ulcerative colitis in a Pseudo Germ-Free animal model. *Biomedicines* **12** <https://doi.org/10.3390/biomedicines12010043> (2023).
17. Kennedy, E. A., King, K. Y. & Baldrige, M. T. Mouse microbiota models: comparing Germ-Free mice and antibiotics treatment as tools for modifying gut bacteria. *Front. Physiol.* **9**, 1534. <https://doi.org/10.3389/fphys.2018.01534> (2018).
18. Ennamorati, M. et al. Intestinal microbes influence development of thymic lymphocytes in early life. *Proc. Natl. Acad. Sci. U S A.* **117**, 2570–2578. <https://doi.org/10.1073/pnas.1915047117> (2020).
19. Lee, S. H., An, J. H., Lee, H. J. & Jung, B. H. Evaluation of Pharmacokinetic differences of acetaminophen in Pseudo germ-free rats. *Biopharm. Drug Dispos.* **33**, 292–303. <https://doi.org/10.1002/bdd.1799> (2012).
20. Hu, H. et al. Carboxymethylated *abrus cantoniensis* polysaccharide prevents CTX-induced immunosuppression and intestinal damage by regulating intestinal flora and Butyric acid content. *Int. J. Biol. Macromol.* **261**, 129590. <https://doi.org/10.1016/j.jbiomac.2024.129590> (2024).
21. Liang, W. et al. Colonization potential to reconstitute a microbe community in Pseudo Germ-Free mice after fecal microbe transplant from equol producer. *Front. Microbiol.* **11**, 1221. <https://doi.org/10.3389/fmicb.2020.01221> (2020).
22. Wichmann, A. et al. Microbial modulation of energy availability in the colon regulates intestinal transit. *Cell. Host Microbe.* **14**, 582–590. <https://doi.org/10.1016/j.chom.2013.09.012> (2013).
23. Agus, A., Clement, K. & Sokol, H. Gut microbiota-derived metabolites as central regulators in metabolic disorders. *Gut* **70**, 1174–1182. <https://doi.org/10.1136/gutjnl-2020-323071> (2021).
24. Baars, A. et al. Sex differences in lipid metabolism are affected by presence of the gut microbiota. *Sci. Rep.* **8**(1), 13426. <https://doi.org/10.1038/s41598-018-31695-w> (2018).
25. Zeng, S. L. et al. Citrus polymethoxyflavones attenuate metabolic syndrome by regulating gut Microbiome and amino acid metabolism. *Sci. Adv.* **6**, eaax6208. <https://doi.org/10.1126/sciadv.aax6208> (2020).
26. Chassaing, B. et al. Dietary emulsifiers impact the mouse gut microbiota promoting colitis and metabolic syndrome. *Nature* **519**, 92–96. <https://doi.org/10.1038/nature14232> (2015).
27. Zhao, J. et al. New insights into the interplay between autophagy, gut microbiota and insulin resistance in metabolic syndrome. *Biomed. Pharmacother.* **176**, 116807. <https://doi.org/10.1016/j.biopha.2024.116807> (2024).
28. Chen, C. Y., Chen, J., He, L. & Stiles, B. L. PTEN: tumor suppressor and metabolic regulator. *Front. Endocrinol. (Lausanne)* **9**, 338. <https://doi.org/10.3389/fendo.2018.00338> (2018).
29. He, F. et al. Resistin regulates fatty acid β oxidation by suppressing expression of peroxisome proliferator activator receptor Gamma-Coactivator 1 α (PGC-1 α). *Cell. Physiol. Biochem.* **46**(5), 2165–2172. <https://doi.org/10.1159/000489546> (2018).
30. Pawlak, M., Lefebvre, P. & Staels, B. Molecular mechanism of PPAR α action and its impact on lipid metabolism, inflammation and fibrosis in non-alcoholic fatty liver disease. *J. Hepatol.* **62**(3), 720–733. <https://doi.org/10.1016/j.jhep.2014.10.039> (2015).

31. Wang, C. et al. PGC-1 α protects against hepatic ischemia reperfusion injury by activating PPAR α and PPAR γ and regulating ROS production. *Oxid. Med. Cell. Longev.* **2021**, 6677955. <https://doi.org/10.1155/2021/6677955> (2021).
32. Avraham, O. et al. Satellite glial cells promote regenerative growth in sensory neurons. *Nat. Commun.* **11**(1), 4891. <https://doi.org/10.1038/s41467-020-18642-y> (2020).
33. Yu, H., Pei, D., Chen, L., Zhou, X. & Zhu, H. Identification of key genes and molecular mechanisms associated with dedifferentiated liposarcoma based on bioinformatic methods. *Onco Targets Ther.* **10**, 3017–3027. <https://doi.org/10.2147/OTT.S132071> (2017).
34. Li, O. et al. *Lactococcus petauri* LZys1 modulates gut microbiota, diminishes ileal FXR-FGF15 signaling, and regulates hepatic function. *Microbiol. Spectr.* **13**(6), e0171624. <https://doi.org/10.1128/spectrum.01716-24> (2025).
35. Araújo, J. R. et al. Fermentation products of commensal bacteria alter enterocyte lipid metabolism. *Cell. Host Microbe.* **27**(3), 358–375e7. <https://doi.org/10.1016/j.chom> (2020).
36. Dhami-Shah, H. et al. Picroside II attenuates fatty acid accumulation in HepG2 cells via modulation of fatty acid uptake and synthesis. *Clin. Mol. Hepatol.* **24**(1), 77–87. <https://doi.org/10.3350/cmh.2017.0039> (2018).
37. Song, S. et al. Peroxisome proliferator activated receptor alpha (PPAR α) and PPAR gamma coactivator (PGC-1 α) induce carnitine palmitoyltransferase 1A (CPT-1A) via independent gene elements. *Mol. Cell. Endocrinol.* **325**(1–2), 54–63. <https://doi.org/10.1016/j.mce.2010.05.019> (2010).
38. Niu, X. et al. Regulation of PPAR γ /CPT-1 expression ameliorates cochlear hair cell injury by regulating cellular lipid metabolism and oxidative stress. *Mol. Genet. Genomics.* **298**(2), 473–483. <https://doi.org/10.1007/s00438-023-01993-8> (2023).

Acknowledgements

The authors gratefully acknowledge Sichuan Heijinshen Sunshine Agriculture Co., Ltd. (Sichuan, China) for providing samples for this study.

Author contributions

Conceptualization, Meixia Wan and Shu Wang; Data curation, Meixia Wan and Qianya Lei; Formal analysis, Meixia Wan, Yudie Xiao and Qianya Lei; Funding acquisition, Meixia Wan and Shu Wang; Investigation, Meixia Wan, Qing Li and Dan Zhou; Methodology, Qing Li, Yudie Xiao and Dan Zhou; Project administration, Meixia Wan, Yudie Xiao, Dan Zhou and Qianya Lei; Visualization, Yudie Xiao and Dan Zhou; Writing – original draft, Meixia Wan and Qing Li; Writing – review & editing, Meixia Wan, Qing Li and Shu Wang. All authors reviewed the manuscript.

Funding

This research was funded by the Sichuan Province Science and Technology Support Program (key research and development program, grant number 2020YFS0031), the Science and Technology Planning Project of Gansu Province (21JR11RM044), the Gansu Provincial University Young Doctoral Support Project (grant number 2024QB-120), the Ph.D. Foundation Program of Long Dong University, China (grant number XYBYZK2310).

Declarations

Competing interests

The authors declare no competing interests.

Ethical approval

The animal study protocol was approved by the Ethics Committee of Sichuan University (protocol code: SYXK (Chuan) 2018-113).

Additional information

Supplementary Information The online version contains supplementary material available at <https://doi.org/10.1038/s41598-025-13715-8>.

Correspondence and requests for materials should be addressed to M.W.

Reprints and permissions information is available at www.nature.com/reprints.

Publisher's note Springer Nature remains neutral with regard to jurisdictional claims in published maps and institutional affiliations.

Open Access This article is licensed under a Creative Commons Attribution-NonCommercial-NoDerivatives 4.0 International License, which permits any non-commercial use, sharing, distribution and reproduction in any medium or format, as long as you give appropriate credit to the original author(s) and the source, provide a link to the Creative Commons licence, and indicate if you modified the licensed material. You do not have permission under this licence to share adapted material derived from this article or parts of it. The images or other third party material in this article are included in the article's Creative Commons licence, unless indicated otherwise in a credit line to the material. If material is not included in the article's Creative Commons licence and your intended use is not permitted by statutory regulation or exceeds the permitted use, you will need to obtain permission directly from the copyright holder. To view a copy of this licence, visit <http://creativecommons.org/licenses/by-nc-nd/4.0/>.

© The Author(s) 2025